Flight Controls: 5513-001
Project: Orbital Control Law

Evan Blosser, OU ID: 113489794

May 22, 2025

1 Introduction

The asteroid 1950DA designated (29075), is a potentially hazardous asteroid (PHA) with a close approach of only 0.05 AU to Earth in 2001, and an impact probability of 2.5×10^{-4} in 2880 [1,2]. The prograde model derived from radar imagining is the one in particular that shows a non-zero impact probability [3]. This serves as grounds for the preliminary mission design for 1950DA to deter it as a possible threat to Earth in the future.

Asteroids like 1950DA carry a significant uncertainty about their nature as we view them from afar. Until a target is visited by a spacecraft, taking detailed scans of the surface and analyzing the composition of samples, the model can only be made as an approximation. This is not the end of the mission, as on approach to the asteroid it can be treated as a point mass. Figure 1 reinforces this notion that we are able to approach the asteroid using a simplistic model as we see the point mass approximation does not deviate significantly from either detailed model at a distance.

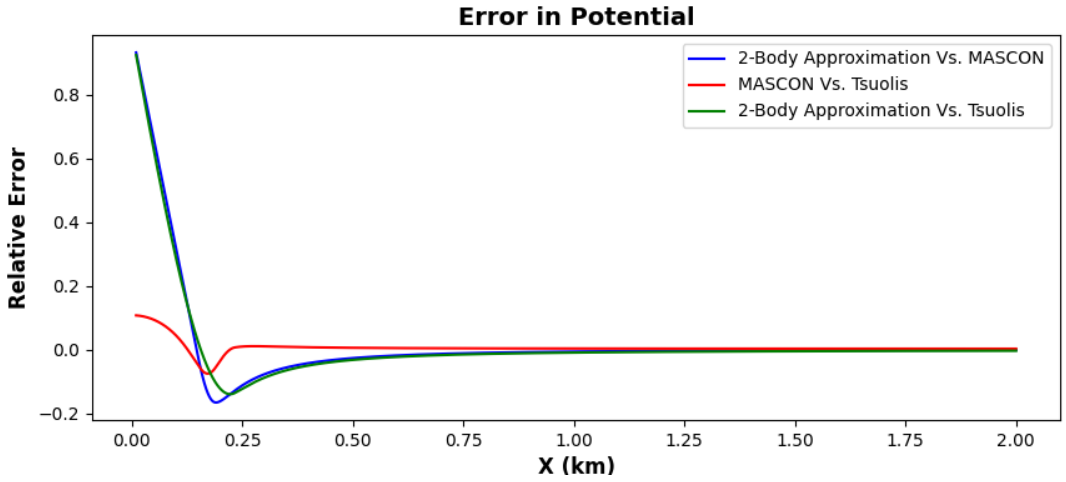

Fig. 1: Relative error in the gravitational potential calculated using: Tsoulis Polyhedron model (Accepted by Industry), MASCON (This work), and the point mass 2-body approximation.

The most recent analysis of 1950DA has led to a minimum Bulk density of 1.7 ± 0.7 g cm^{-3} and a mass of $2.1 \times 10^{12} \pm 1.1$ kg [4]. During the initial analysis, a rough calculation of the volume was conducted and presented as 0.82 km^3 ($\pm 30\%$) [3]. For this work, modeling led to a finding of a scaling factor of $\gamma \approx 0.99137$ (defined in the following section). Table 1 shows the parameters used during this work's modeling process of 1950DA. It can be noted that these parameters are well within the large uncertainty given for the accepted values.

Table 1: Asteroid Parameters			
M	$2.1 \times 10^{12}\ kg$	V	$0.797895\ km^3$
ρ	$2.4 \times 10^{12}\ \frac{kg}{km^3}$	μ	$1.27809 \times 10^{-7}\ \frac{km^3}{s^2}$

1.1 Problem Statement

The problem we face is that the high energy of $H = 3.0 \times 10^{-6}\ \frac{km^2}{s^2}$ with an initial position of $y_0 = 3.0\ km$ inevitably leads to an escape trajectory from the asteroid. This energy is close to a region of bounded motion at $H = 0.1 \times 10^{-6}\ \frac{km^2}{s^2}$. Application of a control law to stabilize the high energy orbit could be beneficial for efficient scanning of the asteroid. This serves as a critical mission step, as most models derived from light curve inversion and Earth-based radar imagining yield in-accurate models. The only detailed models can be made from a close proximity scan of the asteroid. For this reason, most asteroids are scanned and re-evaluated during missions. This feeds into making the orbit solution more refined for a desired spacecraft trajectory. Utilizing a controlled fast orbit could make detailed scans highly efficient saving propellant for other operations.

Rodolfo Batista Negri and Antônio F. B. A. Prado developed a robust path-following control law for Keplerian orbits; applying it to the spacecraft approximations for (99942) Apophis [5]. This path-following control utilizes a desired orbit geometry and is ideal compared to reference tracking for this problem. Instead of relying on time parameterization, this control law defines a sliding surface that uses a virtual arc-length $\vec{y}_d(\theta)$ [6]. This is ideal for our problem as the law allows us to define a specific eccentricity and angular momentum for the spacecraft to follow, and specify the ΔV requirements for the controlled orbit.

2 MASCON-System

Our system is a body-fixed rotating frame orbiting particle of an asteroid. The asteroid model is comprised of MASCON, which represent the center of mass (CM) of each tetrahedron of the polyhedron shape model for the asteroid. The analysis of the gravitational potential of the MASCON model is derived from the theory of the potential in which we treat it as an N-body problem [7]. The attraction of an m_i particle system on a single m_0 particle can be described as the summation of forces, or vectors describing the attractions, of the m_i particles; for $i = 1, 2, \ldots, N$. In this regard, we are treating the external orbiting particle as our m_0, and the m_i masses as our MASCON model for N number of tetrahedron CMs. The gravitational potential is shown below, along with the Jacobian which describes the acceleration imparted to the orbiting particle due to the asteroid's gravitational influence.

$$U = \sum_{i=1}^{N} \frac{\mu_i}{r_i} \tag{1}$$

$$U_\xi = -\sum_{i=1}^{N} \frac{\mu_i r_{\xi_i}}{r_i^3} \qquad U_\eta = -\sum_{i=1}^{N} \frac{\mu_i r_{\eta_i}}{r_i^3} \qquad U_\zeta = -\sum_{i=1}^{N} \frac{\mu_i r_{\zeta_i}}{r_i^3}$$

Where:

- $R_i(x, y, z) = Tetra_{CM}(x, y, z) - Poly_{CM}(x, y, z)$
- $\xi = x_p - R_i(x)$, $\eta = y_p - R_i(y)$, $\zeta = z_p - R_i(z)$
- $r_i = \sqrt{\xi_i^2 + \eta_i^2 + \zeta_i^2}$

We define μ_i as the calculated gravitational parameter for each m_i MASCON, calculated as:

$$\mu_i = Gm_i = G(\rho\gamma V_i).$$

taking Newton's gravitational constant to be $G = 6.67430 \times 10^{-20}\ \frac{km^3}{kg \cdot s^2}$. Here we introduce a scaling factor γ to tie the non-dimensionality of the asteroid's shape model, in Alias Waveform Format (OBJ), to the volume

of each tetrahedron. This gives dimensional units to the model and gives room to remodel the asteroid as new data is taken to solidify key parameters.

The Coriolis and centrifugal forces are present within the XY-plane as the asteroid, like most, is assumed to be spinning about the z-axis. This is a fair and accurate assumption until closer observation of the target, usually by sending a satellite to visit the asteroid. Here we define the equations of motion for the system:

$$\begin{aligned}\ddot{x} =& \omega^2 x + \omega\dot{y} + U_\xi \\ \ddot{y} =& \omega^2 y - \omega\dot{x} + U_\eta \\ \ddot{z} =& U_\zeta\end{aligned}$$

The state matrix representation of this within the code can take a 7×7 form, and our x, as follows:

$$A = \begin{bmatrix} 0 & 0 & 0 & 1 & 0 & 0 & 0 \\ 0 & 0 & 0 & 0 & 1 & 0 & 0 \\ 0 & 0 & 0 & 0 & 0 & 1 & 0 \\ \omega^2 & 0 & 0 & 0 & \omega & 0 & U_\xi \\ 0 & \omega^2 & 0 & -\omega & 0 & 0 & U_\eta \\ 0 & 0 & 0 & 0 & 0 & 0 & U_\zeta \\ 0 & 0 & 0 & 0 & 0 & 0 & 0 \end{bmatrix} \qquad x = \begin{bmatrix} x \\ y \\ z \\ \dot{x} \\ \dot{y} \\ \dot{z} \\ 1 \end{bmatrix}.$$

It can be seen that the matrix $A \in \mathbb{R}^{7\times7}$ has a null state at the bottom to keep the matrix square while we include the gravitational force from the N-body into the system. From this, we can then use the following form to apply the control law discussed in the following section, and allow for integration in Python's `solve_ivp()` integrator.

$$\dot{x} = Ax + Bu$$
$$\Downarrow$$

$$\underbrace{\begin{bmatrix} \dot{x} \\ \dot{y} \\ \dot{z} \\ \ddot{x} \\ \ddot{y} \\ \ddot{z} \\ 0_{null\text{-}state} \end{bmatrix}}_{\dot{x}} = \underbrace{\begin{bmatrix} 0 & 0 & 0 & 1 & 0 & 0 & 0 \\ 0 & 0 & 0 & 0 & 1 & 0 & 0 \\ 0 & 0 & 0 & 0 & 0 & 1 & 0 \\ \omega^2 & 0 & 0 & 0 & \omega & 0 & U_x \\ 0 & \omega^2 & 0 & -\omega & 0 & 0 & U_y \\ 0 & 0 & 0 & 0 & 0 & 0 & U_z \\ 0 & 0 & 0 & 0 & 0 & 0 & 0 \end{bmatrix}}_{A} \cdot \underbrace{\begin{bmatrix} x \\ y \\ z \\ \dot{x} \\ \dot{y} \\ \dot{z} \\ 1 \end{bmatrix}}_{x} + \underbrace{\begin{bmatrix} 0 & 0 & 0 \\ 0 & 0 & 0 \\ 0 & 0 & 0 \\ 1 & 0 & 0 \\ 0 & 1 & 0 \\ 0 & 0 & 1 \\ 0 & 0 & 0 \end{bmatrix}}_{B} \cdot \underbrace{\begin{bmatrix} u_1 \\ u_2 \\ u_3 \end{bmatrix}}_{u}$$

Here we see the terms U_R, U_T, and U_N representing the acceleration corrections designed by the control law used for orbital tracking.

2.1 Simulation and Hamiltonian Mechanics

Near small-bodies like asteroids, classical orbital elements fail, making the ideal choice for the mechanics to be Hamiltonian. Using the following equation for Hamiltonian energy we solve for the velocity of our particle using the assumption that we are setting off from the y-axis in the positive x-direction with a positive $\dot{x}$ velocity. Thus we assume that $\dot{y} = \dot{z} = x = z = 0$:

$$H = \frac{1}{2}(\dot{x}^2 + \dot{y}^2 + \dot{z}^2) - \frac{1}{2}\omega^2(x^2 + y^2) - U$$

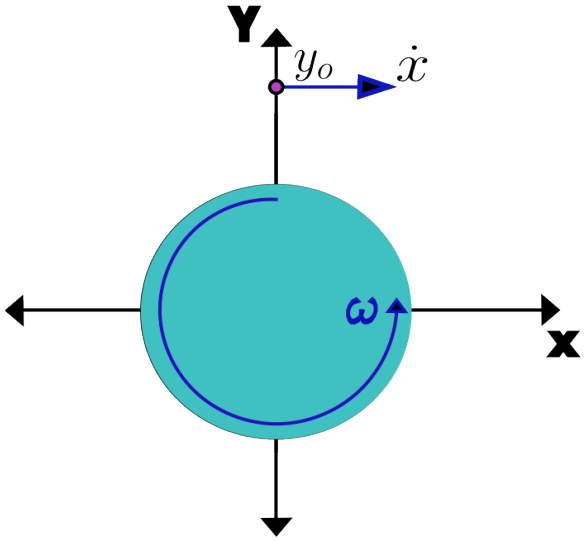

Fig. 2: Depiction of initial orbital orientation. We have the asteroid rotating in a prograde motion relative to the solar system, and the particle orbiting the asteroid in a retrograde motion.

where we define U as the pseudo potential from Eq. (1), solving for the velocity yields:

$$\dot{x} = \sqrt{2H + \omega^2 y_o^2 + 2U}.$$

The diagram in Fig. 2 depicts our orbit with the initial conditions given, we see the asteroid rotates in a prograde motion, with $\omega = 2.1216 \pm 0.00004 \ \frac{rot}{hrs}$ [3]. Thus we are setting the particle to orbit in a retrograde motion about 1950DA. This gives our initial conditions for the system as: $x_o = \begin{bmatrix} 0 & y_0 & 0 & \dot{x} & 0 & 0 \end{bmatrix}^T$.

3 Negri-Prado Robust Path-following Control Law

As discussed previously the path-following algorithm is not parameterized by time, but rather by the virtual arc length making it ideal for controlling Keplerian orbits. In summary, this control law relies solely on the definition of the desired eccentricity and angular momentum vectors defined in the 2-Body problem [6]. This creates a sliding mode control (SMC) law for our non-linear dynamical system applicable to a wide range of orbital station-keeping missions; examples presented by the authors of the control law include the OSIRIS-REx [6, 8]. The control law defines acceleration corrections in the radial-transverse-normal (RTN) frame $\vec{u}_{RTN}$ for any Keplerian orbit, thus we can apply it to our system. This is due to the RTN frame definition, which as defined in the body fixed $(\hat{i}, \hat{j}, \hat{k})$ coordinates of an orbiting target [9]. To begin the definition of the controller we start with the eccentricity vector and the desired orbital angles: Ω_d Longitude of the Ascending Node, ω_d Argument of the Perigee, and i_d inclination.

$$\vec{e}_d = e_d \cdot \begin{bmatrix} \cos\Omega_d \cos\omega_d - \sin\Omega_d \sin\omega_d \cos i_d \\ \sin\Omega_d \cos\omega_d - \cos\Omega_d \sin\omega_d \cos i_d \\ \sin\omega_d \sin i_d \end{bmatrix}$$

Here we see the desired eccentricity vector $\vec{e}_d$ defined, along with the e_d term to help control the desired eccentricity, especially when all angles are set to zero. As can be seen if this is the case then $\vec{e}_d$ will become 1, which defines a parabolic orbit on the verge of becoming a hyperbolic escape trajectory. This form is presented in equation 12 of *"Autonomous and Robust Orbit-Keeping for Small-Body Missions"* [8]. Next, we define the desired angular momentum vector $\hat{h}_d$ as:

$$\hat{h}_d = \begin{bmatrix} \sin i_d \sin \Omega_d \\ -\sin i_d \cos \Omega_d \\ \cos i_d \end{bmatrix}.$$

Utilizing the desired eccentricity and angular momentum vectors the sliding surface $\vec{S}$ is defined as follows:

$$\vec{S} = \begin{bmatrix} (\vec{e} - \vec{e}_d) \cdot (\lambda_R \hat{r} + \hat{\theta}) \\ h - h_d \\ \hat{h}_d \cdot (\lambda_N \hat{r} + \hat{\theta}) \end{bmatrix}.$$

Here we also introduce the control terms λ_R and λ_N as design parameters which help define the convergence to the sliding surface [8]. It can be seen that the difference between the current eccentricity vector with the desired eccentricity vector defines the sliding surface. The same is true for the magnitudes of the current and desired angular momentum vector. As will be discussed later this means $\vec{S}$ must be included in the definition for the equations of motion. Next we define the matrices F and G, used to calculate the acceleration corrections:

$$F = \frac{1}{h\mu} \begin{bmatrix} -h^2 & (2\lambda_R h - (\dot{\vec{r}} \cdot \hat{r})r)h & -\mu r \vec{e}_d \cdot \hat{h} \\ 0 & \mu r h & 0 \\ 0 & 0 & \mu r \hat{h}_d \cdot \hat{h} \end{bmatrix}$$

$$G = \frac{h}{r^2} \begin{bmatrix} (\vec{e} - \vec{e}_d) \cdot (\lambda_R \hat{\theta} - \hat{r}) \\ 0 \\ \hat{h}_d \cdot (\lambda_N \hat{\theta} - \hat{r}) \end{bmatrix}$$

These matrices carry two main assumptions, the first being that the magnitudes of the position vector $\vec{r}$ and angular momentum vector $\vec{h}$ are not zero. The second is that far a given angle β, defined as $\cos\beta = \hat{h} \cdot \hat{h}_d$, must be bound as under $\frac{\pi}{2}$ or $\beta < 90^\circ$. If these assumptions remain true then the matrix F is always invertible. The event that these assumptions would be invalid is rare in station keeping as this would either be a non-moving target, or too chaotic of a trajectory respectively. An algorithm is presented to circumvent these matrices if needed for $\beta \geqslant 90^\circ$ [8]. The saturation function, used in the controller, is defined as follows:

$$sat(\alpha, \beta) = \begin{cases} +1 & \alpha > \beta \\ \frac{\alpha}{\beta} & -\beta \leqslant \alpha \leqslant \beta \\ -1 & \alpha < -\beta \end{cases}.$$

The saturation function itself helps to saturate the controller with values of 1 or -1 depending on the given parameters. It is used in SMC to avoid discontinuous control inputs, yielding a convergences boundary for the sliding surface at some performance costs [8]. Here we define the gain matrix K and the Φ design matrix utilized by the saturation function to control the input for the sliding surface $\vec{s}$:

$$\Phi = \begin{bmatrix} d_R \\ d_T \\ d_N \end{bmatrix} = n_\Phi diag(K) \qquad K = \begin{bmatrix} k_{11} & 0 & 0 \\ 0 & k_{22} & 0 \\ 0 & 0 & k_{33} \end{bmatrix}.$$

The parameter n_Φ is defined to select the size of the boundary about the sliding surface and is used for creating the control matrix Φ from the gain matrix K. The gain matrix K also carries with it inequalities that help specify its design to the system. They are presented with the terms D_R, D_T, D_N representing the

disturbance matrix terms in the RTN frame. The inequalities are as follow:

$$k_{11} \geqslant \frac{h}{\mu} D_R + \left| \frac{2\lambda_R h - (\dot{\vec{r}} \cdot \hat{r}) r}{\mu} \right| D_T + \frac{r \left| \hat{e}_d \cdot \hat{h} \right|}{h} D_N$$
$$k_{22} \geqslant r D_T$$
$$k_{33} \geqslant r \frac{\hat{h}_d \cdot \hat{h}}{h} D_N$$

The disturbance matrices are the approximation of the knowns and unknowns of the system. The disturbance due to the spin state in the body frame is an example of an unknown [8]. Using the F, G, K, Φ matrices along with the sliding surface $\vec{s}$ and the saturation function, we now define the equation for the acceleration corrections as:

$$\vec{u}_{RTN} = -F^{-1}(G + Ksat(\vec{s}, \Phi)) = \begin{bmatrix} U_R \\ U_T \\ U_N \end{bmatrix} \tag{2}$$

We then use the following relation to rotate the corrections into our reference frame:

$$\vec{u} = U_R \hat{r} + U_T \hat{\theta} + U_N \hat{h} = \begin{bmatrix} u_1 \\ u_2 \\ u_3 \end{bmatrix} \tag{3}$$

Where we define the unit vectors of the RTN frame as follows:

$$\hat{r} = \frac{\vec{r}}{\|\vec{r}\|} \qquad \hat{h} = \frac{\vec{h}}{\left\|\vec{h}\right\|} \qquad \hat{\theta} = \hat{h} \times \hat{r}$$

The position and velocity vector is defined within the state vector x:

$$\vec{r} = \begin{bmatrix} x & y & z \end{bmatrix}^T \qquad \dot{\vec{r}} = \begin{bmatrix} \dot{x} & \dot{y} & \dot{z} \end{bmatrix}^T$$

which are used to calculate the eccentricity and angular momentum vectors as follows:

$$\vec{e} = \frac{1}{\mu}(\dot{\vec{r}} \times \vec{h} - \mu \hat{r}) \qquad \vec{h} = \vec{r} \times \dot{\vec{r}}$$

3.1 Designing the Controller:

Equation (3) is used as our systems control input u for the integration of the system $\dot{x} = Ax + Bu$. Yet one key part of the design of this control law is to define specific parts of the controller inside the equations of motion being integrated. This is because for each integration step new eccentricity and momentum vectors ($\vec{e}$ & $\vec{h}$) will need to be calculated to define the error between the current and desired eccentricity and angular momentum vectors.

The sliding surface $\vec{S}$ along with the F and G matrices are all defined within the equations to be integrated and are solved for with each step. This is because they contain various terms for the difference between the desired and current eccentricity and angular momentum vectors. These are then used to calculate the acceleration corrections $\vec{u}_{RTN}$. As can be seen in the source code, The gain matrix K along with Φ, and the disturbance matrix D, all need to be designed for the system initially, thus they are outside of the equation of motion definition.

For the design of the disturbance matrix D, we can hold the assumption that $D = D_R = D_T = D_N$. In practice, the disturbance matrix can be chosen, relative to the units and order of magnitude as the total gravitational acceleration in the body fixed rotating frame. In this regard, we base our choice on the disturbances at our initial position when calculating the velocity as shown in Table 2.

Table 2: Disturbance Matrix Approximation					
H	$3.0 \times 10^{-6}\ \frac{km^2}{s^2}$	U_{Pseudo}	$4.26962 \times 10^{-8}\ \frac{km^2}{s^2}$	Centri. Force	$7.30915 \times 10^{-6}\ \frac{km^2}{s^2}$

Using the initial conditions of $H = 3.0 \times 10^{-6}\ \frac{km^2}{s^2}$ and $y_0 = 3.0\ km$, the rough estimation of the centrifugal force can be made, which aids in designing of the D and subsequent matrices. Thus our selection of $\approx 1 \times 10^{-14}$, shows we want our ΔV corrections to be in the order of m^2 while remaining in km units and within the same order of magnitude as the known forces.

3.2 Initial Controller settings:

The disturbance matrix was set as follows:

$$D = \begin{bmatrix} 1.0 \times 10^{-14} \\ 1.0 \times 10^{-14} \\ 1.0 \times 10^{-14} \end{bmatrix}$$

which then defining the gain and Φ matrices, with adjustment parameters for the inequality $k_{11}, k_{22}, k_{33} = 1 \times 10^{11}$, yielding the following:

$$K = \begin{bmatrix} 2.87 \times 10^{-10} & 0 & 0 \\ 0 & 1.003 \times 10^{-11} & 0 \\ 0 & 0 & 1.00846 \times 10^{-11} \end{bmatrix} \qquad \Phi = \begin{bmatrix} 2.8718 \times 10^{-10} \\ 1.003 \times 10^{-11} \\ 1.00846 \times 10^{-11} \end{bmatrix}.$$

Parameters: $\lambda_R = \lambda_N = 0.02$, $n_\Phi = 1.0$ with all angles set to zero; $i_d = 0^\circ$, $\Omega_d = 0^\circ$, $\omega_d = 0^\circ$ we set $e_d = 0.005$, to define a circular orbit at an approximate zero eccentricity. This is key as the defined orbit has too low of an altitude to make a parabolic orbit without the dangers of low altitude passes causing a collision with the asteroid.

4 Results

Figure 3 & 4 show the results of the Negri-Prado SMC law effectively controlling the orbiting particle from the escape trajectory. The limit of escape is taken as the hill's radius multiplied by 5 to ensure no, calculated as $R_H = R(\frac{m_{body}}{M_\odot})$.

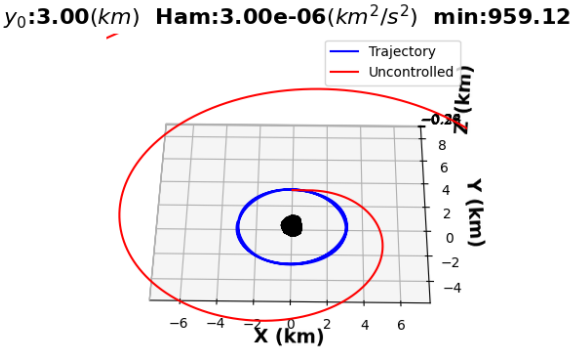

Fig. 3: Comparison of controlled versus the uncontrolled escape trajectory.

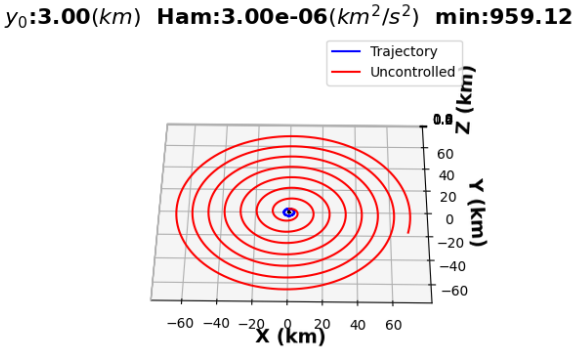

Fig. 4: Expanded comparison view.

For the asteroid 1950DA $R_H \approx 14.46513$ km, thus the limit of escape is ≈ 72.32565 km. This magnification of the hill sphere is due to its theoretical definition. There could exist possible return trajectories that

cross this boundary, yet don't escape from the asteroid's gravitational influence. The ΔV used was by the control inputs was $\approx 0.00133841\ km/s$ or $1.33841\ m/s$. Figure 11 shows that the controlled orbit is a proper Keplerian orbit. We can see that the velocity reaches a maximum at perigee, and minimum at apogee as expected. Furthermore, the Hamiltonian energy can be seen to decrease as our velocity increases and increases as it decreases storing the energy in the potential energy portion of the Hamiltonian energy.

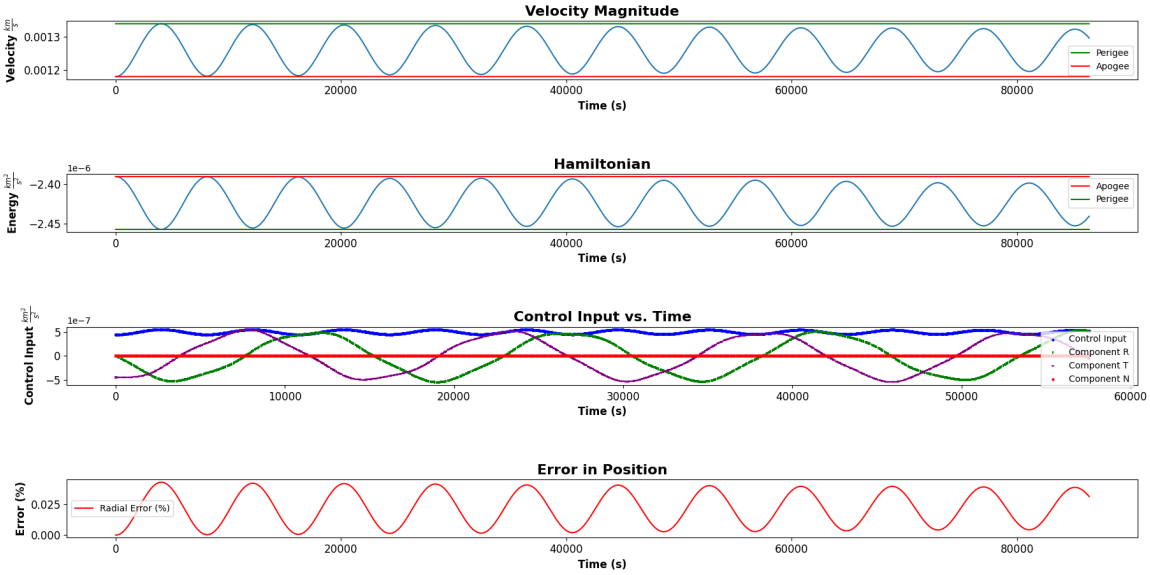

Fig. 5: Velocity, Hamiltonian energy, control input, and radial error data from the comparison. The particle escaped after ≈ 15.985 hours ending the simulation.

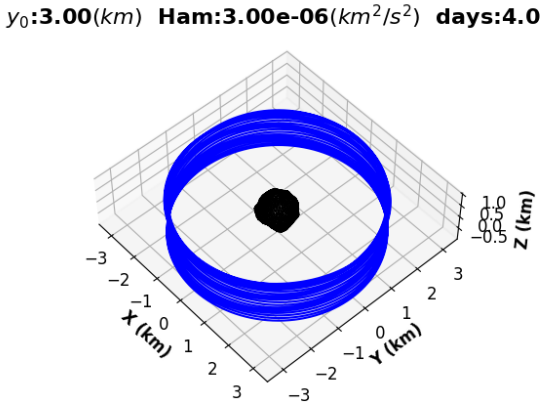

Fig. 6: 4-Day orbit, initial position $y = 3.0\ km$ and $z = 0.6\ km$.

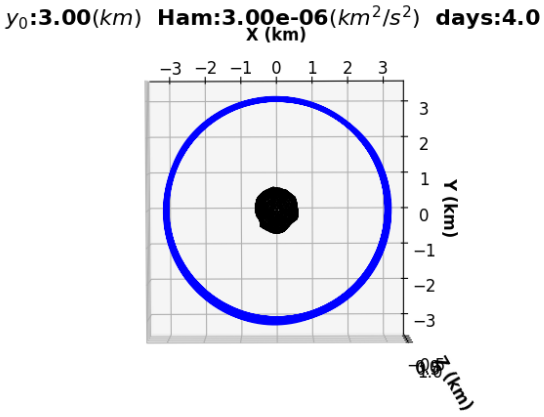

Fig. 7: Top view of 4-Day orbit

The orbit shown in Fig. 6 - 7 utilized a minimum ΔV of $\approx 0.00755313\ km/s$ or $7.55313\ m/s$ for a total of 4 days and as can be seen the orbit's structure spans the surface of the asteroid, making it an ideal orbit for reconnaissance prior to surface landing. Examining Fig. 8, we can see the Hamiltonian energy slowly decreasing over time, which is also reflected in the decrease in average velocity. These irregularities as compared to the center orbit are due to the control input which can be seen to reach a maximum when

the velocity does. This reflects the controller trying to decrease the high energy, especially at the peak to ensure the orbit converse to the sliding surface rather than escaping. Starting from $y_o = 3.0\ km$ and an added initial height of$z_o = 0.6\ km$, and allowing it to develop for a period of 4 days, the orbit is controlled in a circular motion down the length of the asteroid relative to the z-axis. By analyzing the Hamiltonian energies behavior we can see that the controller ended up decreasing the energy significantly despite the high initial energy given to the orbiting particle.

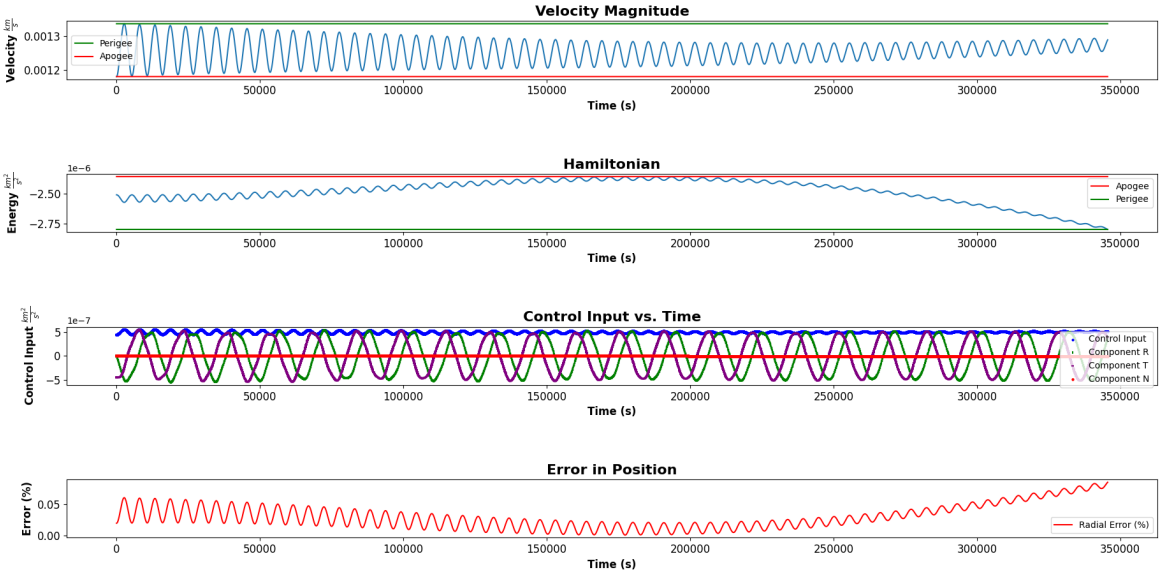

Fig. 8: Velocity, Hamiltonian energy, control input, and radial error data from the 4-Days of orbit.

5 Fine Tuning the Negri-Prado SMC Law

Adjusting the λ_N parameter, inherently linked to the normal component, as can be seen in the definition of the F and G matrices, λ_N takes the N position of the RTN frame.

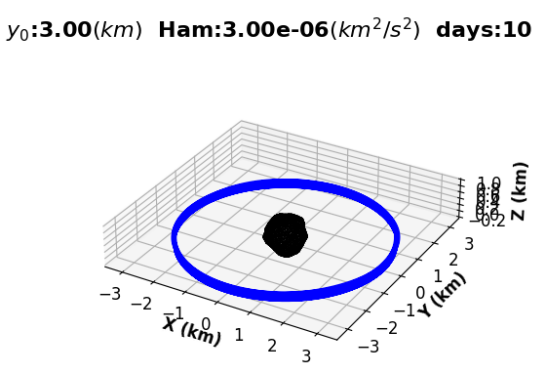

Fig. 9: 10-Day orbit.

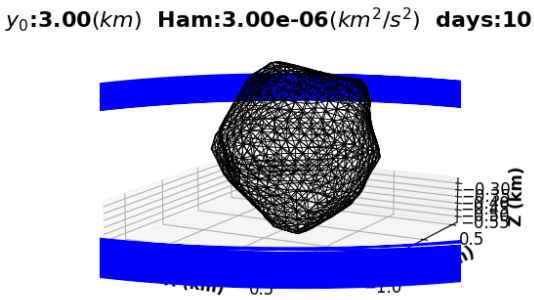

Fig. 10: Close up to show the density of lines within the quasi-periodic orbit.

Thus increasing $\lambda_N = 0.53$, and $n_\Phi = 10.0$ to allow for optimal performance for the convergences to the sliding surface with minimal error [8]. With this the orbit shown in Fig. 10 was simulated for a total of 10 days and showed a quasi-periodic orbit with minimal z-axis drift. Even though it is ideal for scanning the asteroid, this orbit is ideal for station-keeping during the mission. This was at a cost of $\Delta V \approx 0.01631487\ km/s$ or $\Delta V \approx 16.31487\ m/s$. By increasing the parameter linked to the radial component $\lambda_R = 0.53$ we saw a drastic decrease in the amount of required ΔV to keep this orbit of only $\approx 0.00815897\ km/s$ or $\approx 8.15897\ m/s$.

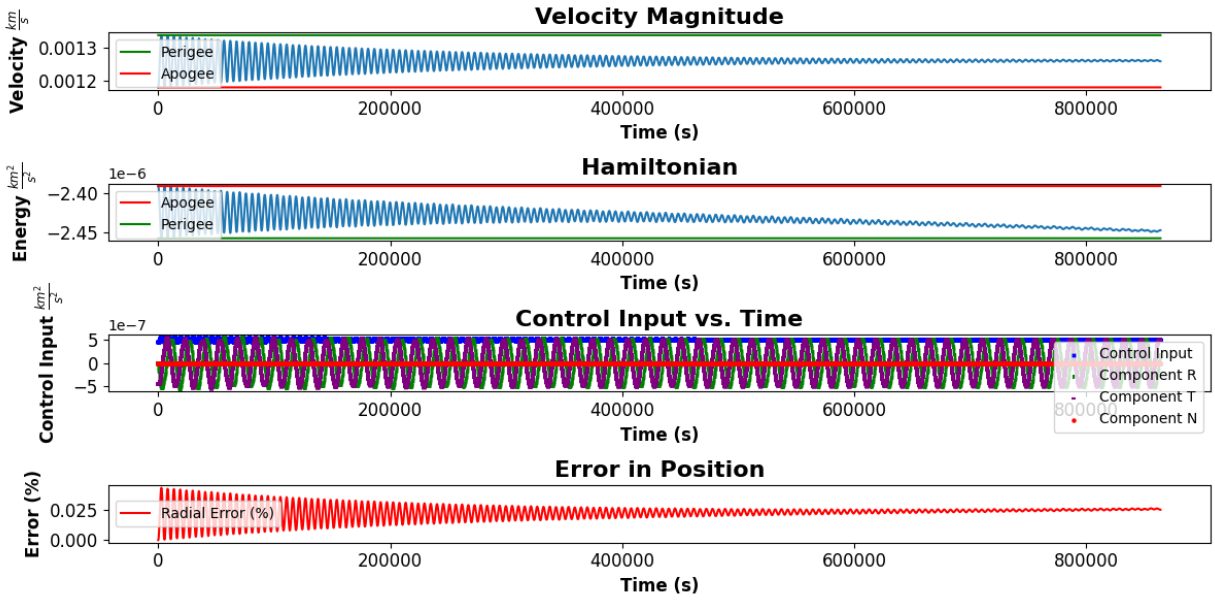

Fig. 11: Velocity, Hamiltonian energy, control input, of 10-Day orbit.

The refinement of the Negri-Prado SMC law settings can be conducted to optimize the required ΔV of either the scanning or station-keeping trajectories. This can also yield other useful orbits for further mission objectives. The key to this controller is the refinement of each chosen parameter with regards to the desired motion. By increasing the λ_N parameter linked to the normal component of the acceleration correction matrices, and subsequently the acceleration correction $\vec{u}$, we see a control of the normal or z orbital direction.

6 Conclusion

The results of the simulations yielded a proper implementation of the Negri-Prado path-following SMC law for Keplerian orbits. The initial comparison showed that after ≈ 15.985 hours, an uncontrolled particle will escape while the SMC shows a required $\Delta V \approx 1.33841\ m/s$ in order to stabilize the particle's motion into a more quasi-periodic like orbit. Allowing the simulation to develop for a period of 4 days with an initial height of $z_o = 0.6\ km$ yielded an orbital motion ideal for scanning the entire asteroid's surface. This could save propellant and resources, given that most spacecraft are already scrutinized for weight reduction this is vital for additional mission operations. The total scanning of 1950DA would require a $\Delta V \approx 7.55313\ m/s$ which is nominal given the high energy of $H = 3.0 \times 10^{-6}\ \frac{km^2}{s^2}$ which would otherwise yield a fast escape trajectory.

By refining the parameters of the control law, a station-keeping trajectory was found to be quasi-periodic in nature and held for 10 days. This was at a cost of $\Delta V \approx 8.15897\ m/s$, and achieved by adjusting the radial and normal component parameters λ_R & λ_N respectively.

Appendix A: Running code

Simply run either `Main_Sim.py` or `Main_Sim_No_Compare.py` in a Python 3 Interactive Development Environment (IDE), to initiate the simulation with the Negri-Prado SMC law. You may need to run the following command to install dependencies:

```
pip install trimesh
```

Appendix B: MASCON Model

Representation of the MASCON model, plotting the OBJ mesh (black grid with blue vertices) around the CM data (in red):

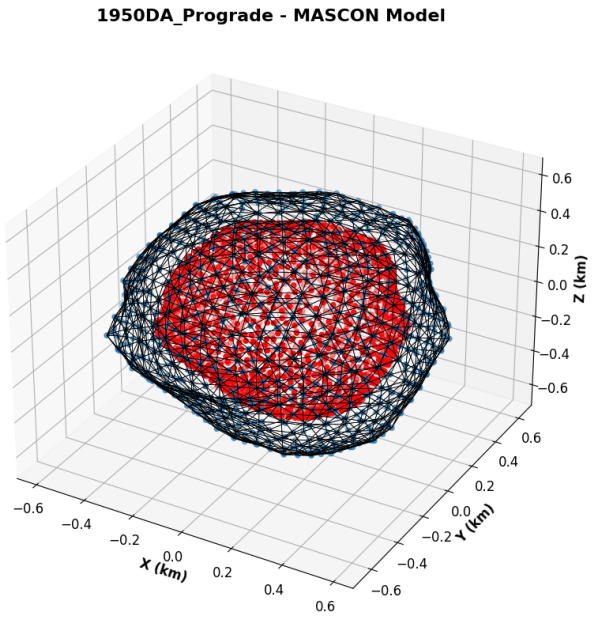

Acronyms

CM center of mass

MASCON Mass Concentration

OBJ Alias Waveform Format

PHA potentially hazardous asteroid

RTN radial-transverse-normal

SMC sliding mode control

References

[1] J. D. Giorgini, S. J. Ostro, L. A. M. Benner, P. W. Chodas, S. R. Chesley, R. S. Hudson, M. C. Nolan, A. R. Klemola, E. M. Standish, R. F. Jurgens, R. Rose, A. B. Chamberlin, D. K. Yeomans, and J.-L. Margot, "Asteroid 1950 da's encounter with earth in 2880: Physical limits of collision probability prediction," *Science*, vol. 296, pp. 132–136, Apr. 2002.

[2] D. Farnocchia and S. Chesley, "Assessment of the 2880 impact threat from asteroid (29075) 1950 da," *Icarus*, vol. 229, pp. 321–327, Feb. 2014.

[3] M. BUSCH, J. GIORGINI, S. OSTRO, L. BENNER, R. JURGENS, R. ROSE, M. HICKS, P. PRAVEC, P. KUSNIRAK, and M. IRELAND, "Physical modeling of near-earth asteroid (29075) 1950 da," *Icarus*, vol. 190, pp. 608–621, Oct. 2007.

[4] B. Rozitis, E. MacLennan, and J. P. Emery, "Cohesive forces prevent the rotational breakup of rubble-pile asteroid (29075) 1950 da," *Nature*, vol. 512, pp. 174–176, Aug. 2014.

[5] S. Aljbaae, D. M. Sanchez, A. F. B. A. Prado, J. Souchay, M. O. Terra, R. B. Negri, and L. O. Marchi, "First approximation for spacecraft motion relative to (99942) apophis," 2020.

[6] R. B. Negri and A. F. B. d. A. Prado, "Robust path-following for keplerian orbits," 2020.

[7] W. D. MacMillan, *The Theory of the Potential*. Dover Publications, Inc., 1958.

[8] R. Batista Negri and A. F. B. A. Prado, "Autonomous and robust orbit-keeping for small-body missions," *Journal of Guidance, Control, and Dynamics*, vol. 45, pp. 587–598, Mar. 2022.

[9] H. Curtis, *Orbital Mechanics for Engineering Students Revised Reprint*. Elsevier Science Technology, 2020.